Anal. Chem. **2008,** *80,* 7651–7660

Articles

Biological/Biomedical Accelerator Mass Spectrometry Targets. 1. Optimizing the CO_2 Reduction Step Using Zinc Dust

Seung-Hyun Kim,[†] Peter B. Kelly,[‡] and Andrew J. Clifford*[,†]

Department of Nutrition and Department of Chemistry, University of California Davis, One Shields Avenue, Davis, California 95616

Biological and biomedical applications of accelerator mass spectrometry (AMS) use isotope ratio mass spectrometry to quantify minute amounts of long-lived radioisotopes such as ^{14}C. AMS target preparation involves first the oxidation of carbon (in sample of interest) to CO_2 and second the reduction of CO_2 to filamentous, fluffy, fuzzy, or firm graphite-like substances that coat a −400-mesh spherical iron powder (−400MSIP) catalyst. Until now, the quality of AMS targets has been variable; consequently, they often failed to produce robust ion currents that are required for reliable, accurate, precise, and high-throughput AMS for biological/biomedical applications. Therefore, we described our optimized method for reduction of CO_2 to high-quality uniform AMS targets whose morphology we visualized using scanning electron microscope pictures. Key features of our optimized method were to reduce CO_2 (from a sample of interest that provided 1 mg of C) using 100 ± 1.3 mg of Zn dust, 5 ± 0.4 mg of −400MSIP, and a reduction temperature of 500 °C for 3 h. The thermodynamics of our optimized method were more favorable for production of graphite-coated iron powders (GCIP) than those of previous methods. All AMS targets from our optimized method were of 100% GCIP, the graphitization yield exceeded 90%, and $\delta^{13}C$ was −17.9 ± 0.3‰. The GCIP reliably produced strong $^{12}C^-$ currents and accurate and precise F_m values. The observed F_m value for oxalic acid II NIST SRM deviated from its accepted F_m value of 1.3407 by only 0.0003 ± 0.0027 (mean ± SE, n = 32), limit of detection of ^{14}C was 0.04 amol, and limit of quantification was 0.07 amol, and a skilled analyst can prepare as many as 270 AMS targets per day. More information on the physical (hardness/color), morphological (SEMs), and structural (FT-IR, Raman, XRD spectra) characteristics of our AMS targets that determine accurate, precise, and high-throughput AMS measurement are in the companion paper.

Accelerator mass spectrometry (AMS) is known for its exquisite sensitivity in quantifying ^{14}C. AMS uses tandem mass spectrometry to quantify long-lived radioisotopes with attomolar sensitivity at a precision of ≤1%. This ability is especially useful in conducting ^{14}C tracer studies in biological/biomedical systems.[1−3] In order for AMS to measure ^{14}C in biologic specimens, they were converted to graphite or possibly a mix of closely related forms of carbon such as amorphous carbon, iron carbide, and graphite (that we characterize in part 2). AMS target preparation begins by first converting sample carbon into carbon dioxide gas and then reducing the CO_2 to graphite that coats over metal catalysts. Previously used reduction methods include thermal and radiofrequency (rf) cracking of hydrocarbon[4,5] and a glow-discharge (DC) in CO/H_2,[6] but now they are not widely used for AMS.

* To whom correspondence should be addressed: E-mail: ajclifford@ucdavis.edu. Tel: 530-752-3376. Fax: 530-752-8966.

[†] Department of Nutrition.

[‡] Department of Chemistry.

(1) Felton, J. S.; Turteltaub, K. W.; Vogel, J. S.; Balhorn, B.; Gledhill, B. L.; Southon, J. R.; Caffee, M. W.; Finkel, R. C.; Nelson, D. E.; Proctor, I. D.; Davis, J. C. *Nucl. Instrum. Methods Phys. Res., Sect. B* **1990**, *52*, 517–523.

(2) Lin, Y.; Dueker, S. R.; Follett, J. R.; Fadel, J. G.; Arjomand, A.; Schneider, P. D.; Miller, J. D.; Green, R.; Buchholz, B. A.; Vogel, J. S.; Phair, R. D.; Clifford, A. J. *Am. J. Clin. Nutr.* **2004**, *80*, 680–691.

(3) Clifford, A. J.; de Moura, F. F.; Ho, C. C.; Chuang, J. C.; Follett, J.; Fadel, J. G.; Novotny, J. A. *Am. J. Clin. Nutr.* **2006**, *84*, 1430–1441.

(4) Wand, J. O.; Gillespie, R.; Hedges, R. E. M. *J. Archaeological Sci.* **1984**, *11*, 159–163.

(5) Beukens, R. P.; Lee, H. W. *Symposium on Accelerator Mass Spectrometry, Proc: Agronne Natl Lab, ANL/PHY-81−1* **1981**, *416*, 425.

(6) Andree, M.; Beer, J.; Oeschger, H.; Bonani, G.; Hofmann, H. J.; Morenzoni, E.; Nessi, M.; Suter, M.; Wölfli, W. *Nucl. Instrum. Methods Phys. Res. Sect. B* **1984**, *5*, 274–279.

10.1021/ac801226g CCC: $40.75
Published on Web 09/12/2008

Currently popular reductants for AMS are H_2 or Zn ($Zn + CO_2 = ZnO + CO$, $Zn + H_2O = ZnO + H_2$) because either reductant produces improved AMS measurements. Use of Zn as a reductant was first reported for carbon dating.[7,8] Time required to reduce CO_2 to graphite using Zn as reductant ranged from 2 to 10 h depending on the sample size, the temperature, and the type and the size of catalyst used. AMS applications in geochronology and archeology typically require great sensitivity and precision but not necessarily a high throughput, while biological/biomedical application of AMS typically requires less sensitivity but accuracy and high throughput are essential.[9−11]

The method for biological/biomedical AMS application[12] used flame-sealed quartz tube containing a mix of Zn dust plus titanium hydride (TiH_2) as reductant. The method also used a disposable CO_2 gas-transfer system to minimize sample-to-sample contamination. High throughput was considered to be ∼60 samples per d/skilled analyst.[12] A recent method used a mix of prebaked TiH_2 and Zn dust to increase sensitivity for radiocarbon dating, but throughput was 40 samples per d/analyst.[13] The flame-sealed quartz tube was replaced with a septa-sealed vial, which increased the throughput to 150 samples per d/skilled analyst.[14] The method[14] used 2−3 mg of −400 mesh spherical Fe powder (−400MSIP), a temperature of 500 °C for 4 h, and the AMS targets made by this method produced a satisfactory ion current but the fraction modern (F_m) values were still variable in our experience. So, we modified the method[14] to mitigate variability in the F_m values by raising the amount of −400MSIP to 10 mg, the temperature to 525 °C, and the time to 6 h. We refer to the modified method as "our previous method".[15] Eighty percent of the time our previous method[15] produced AMS targets of graphite-coated Fe (GCI) and 20% of the time it produced AMS targets of a gray-colored iron−carbon material (ICM) instead of GCI. AMS targets of GCI produced a reliable ion current of ∼115 μA $^{12}C^-$/mg of C while AMS targets of ICM produced an ion current that was only 87% as strong as AMS targets of GCI. Furthermore, AMS targets of ICM and of GCI were hard and consequently were difficult to tamp into AMS target holders. AMS targets of metal carbide, especially cobalt carbide, produced low ion currents with a variability of 5−10% in the accompanying $^{14}C/^{13}C$ ratios.[12] The reliability and variability of ion currents and F_m values along with the limited throughput prompted us to further optimize the preparation of AMS targets[12,14,15] for biological/biomedical applications.

EXPERIMENTAL SECTION

Reagents. The reductant (Zn dust, CAS No. 7440−66−6, <10 μm, 98+ %) was purchased from Sigma-Aldrich (St. Louis, MO). The five catalysts (three of Fe and two of Co) differed from one another in type, particle size, and particle shape. The −400MSIP was from Sigma-Aldrich (CAS No. 7439−89−6, 99.99+ %); it was used as the reference catalyst.[15] The −325 mesh, irregular Fe, H_2 reduced (Catalog No. FE-110, 99.8%) and the −50/+100 mesh, irregular FeH_2 (Catalog No. FE-114, 99.8%) were from Atlantic Equipment Engineers (AEE, Bergenfield, NJ). The two Co catalysts included, the −325 mesh irregular Co (Catalog No. 10456, 99.5%) from Alfa-Aesar (Ward Hill, MA), and the −100 mesh cracked egg shell-like Co (CAS No. 7440−48−4, <150 μm, 99.9+ %) was from Sigma-Aldrich. The four sources of solid/sample C included oxalic acid powder (Ox-2, SRM 4990C), Australian National University sucrose (ANU sucrose), tributyrin (TRIB), and fasting human plasma. The Ox-2 SRM was from National Institute of Standards and Technology (NIST), Gaithersburg, MD. The accepted F_m value for the Ox-2 SRM was 1.3407.[16] Four milligrams of the Ox-2 SRM supplied 1 mg of solid C. The ANU sucrose was from the Lawrence Livermore National Laboratory (LLNL), 2.38 mg supplied 1 mg of solid C. The methanol (MeOH, CAS No. 67−56−1, HPLC grade) was from Fisher-Scientific (Santa Clara, CA). The TRIB (CAS No. 60−01−5, sub-Modern carbon carrier) was from MP Biomedicals (Solon, OH). The TRIB was diluted with MeOH (TRIB/MeOH, 1:24, v:v) so that each 50 μL of TRIB−MeOH solution supplied 1.19 mg of solid C. Fasting human plasma (baseline) was from each of four healthy nonsmoking persons whose ages ranged from 25 to 67 y. A 25-μL aliquot of plasma supplied ∼1 mg of solid C.[17]

Procedure. In optimizing the reduction step of our previous method,[15] Ox-2 was used as the AMS standard rather than the ANU whose supply was limited. Oxidation of the 1-mg aliquots of solid C (which has traces of H_2O vapor) to CO_2 was conducted as described by our previous method.[15] Transfer of the CO_2 to septa-sealed vials that had an inner vial containing a catalyst that sat atop glass beads that sat atop a reductant (Zn dust) was also the same as by our previous method[15] except that several amounts of reductant, catalyst, types of catalysts, heating temperatures, and heating durations were evaluated as summarized in Table 1. Criteria for evaluating the AMS data included a high, reliable, and stable $n^{13}C^+$ current along with an accurate F_m value. The reductant levels ranged from 1 to 300 mg of Zn dust in increments of 25 mg. The five catalysts included three of iron and two of cobalt, each at only one level, 10 mg. Then, six levels of the best performing (defined by ion current) of the five catalysts that ranged from 1 to 10 mg were evaluated. Three reduction temperatures that ranged from 500 to 550 °C in increments of 25 °C and 12 reduction durations that ranged from 0.5 to 6 h in increments of 0.5 h were tested. Graphitization yield and isotopic fractionation were measured using a PDZ Europa ANCA-GSL elemental analyzer interfaced to a PDZ Europa 20−20 isotope ratio mass spectrometer (Sercon Ltd., Cheshire, UK).[18] The resulting graphite was tamped into AMS target holders and analyzed at the LLNL as by our previous method.[15] The $^{13}C^+$ current of the AMS target of interest was normalized by the $^{13}C^+$ current of the Ox-2 SRM and referred to as normalized $^{13}C^+$ ($n^{13}C^+$) current.

(7) Jull, A. J. T.; Donahue, D. J.; Hatheway, A. L.; Linick, T. W.; Toolin, L. J. *Radiocarbon* **1986**, *28*, 191–197.
(8) Slota, P. J.; Jull, A. J. T.; Linick, T. W.; Toolin, L. J. *Radiocarbon* **1987**, *29*, 303–306.
(9) Vogel, J. S.; Turteltaub, K. W.; Finkel, R.; Nelson, D. E. *Anal. Chem.* **1995**, *67*, 353A–359A.
(10) Vogel, J. S.; Turteltaub, K. W. In *Mathematical Modeling in Experimental Medicine and Biology*; Clifford, A. J., Müller, H. G., Eds.; Plenum: New York, 1998; pp 397−410.
(11) Liberman, R. G.; Skipper, P. L.; Prakash, C.; Shaffer, C. L.; Flarakos, J.; Tannenbaum, S. R. *Nucl. Instrum. Methods Phys. Res., Sect. B* **2007**, *259*, 773–778.
(12) Vogel, J. S. *Radiocarbon* **1992**, *34*, 344–350.
(13) Marzaioli, F.; Borriello, G.; Passariello, I.; Lubritto, C.; De Cesare, N.; D'Onofrio, A.; Terrasi, F. *Radiocarbon* **2008**, *50*, 139–149.
(14) Ognibene, T. J.; Bench, G.; Vogel, J. S.; Peaslee, G. F.; Murov, S. *Anal. Chem.* **2003**, *75*, 2192–2196.
(15) Getachew, G.; Kim, S. H.; Burri, B. J.; Kelly, P. B.; Haack, K. W.; Ognibene, T. J.; Buchholz, B. A.; Vogel, J. S.; Modrow, J.; Clifford, A. J. *Radiocarbon* **2006**, *48*, 325–336.
(16) Mann, W. B. *Radiocarbon* **1983**, *25*, 519–527.

Table 1. Factors/Conditions Tested to Optimize Reduction of CO_2 from 1 mg of Solid C to Graphite for AMS

our previous method[15]	100 mg of Zn dust/mg of C, 10 mg of −400MSIP/mg of C, 525 °C, 6 h	Figure 1	replications
reductant mass, Zn dust	1−300 mg of Zn dust (Sigma-Aldrich, CAS No. 7440−66−6, <10 μm, 98+%)/mg of C, increments of 25	Figure 2	≥2
catalyst type	−400MSIP (Sigma-Aldrich, CAS No. 7439−89−6, 99.99+ %)	Figure 3	≥4
iron	−325 mesh irregular Fe, H_2 reduced (Atlantic Equipment Engineers (AEE), Bergenfield, NJ, Cat. No. FE-110, 99.8%)	Figure 3	≥4
		Figure 3	≥4
	−50/+100 mesh irregular Fe, H_2 reduced (AEE, Cat. No. FE-114, 99.8%)	Figure 3	≥4
cobalt	−325 mesh irregular Co (Alfa-Aesar, Ward Hill, MA, Cat. No. 10456, 99.5%)	Figure 3	≥4
	−100 mesh cracked egg shell like Co (Sigma-Aldrich, CAS No. 7440−48−4, < 150 μm, 99.9+ %)	Figure 3	≥4
best catalyst mass	−400MSIP (Sigma-Aldrich, CAS No. 7439−89−6, 99.99+ %), 1, 3, 5, 6.5, 8, and 10 mg/mg of C	Figure 4	≥4
temperatures	500, 525, and 550 °C	Figure 5	≥4
heating times	from 0.5 to 6 h, in increments of 0.5	Figure 6	≥2
our optimized method	100 mg of Zn dust/mg of C, 5 mg of −400MSIP/mg of C, 500 °C, 3 h.	Figure 7	≥32

Oxalic acid II (4 ± 0.3 mg (± SD), F_m value of NIST SRM 4990C that was 1.3407) was oxidized to provide 1 mg of C (as CO_2) as previously described.[16]

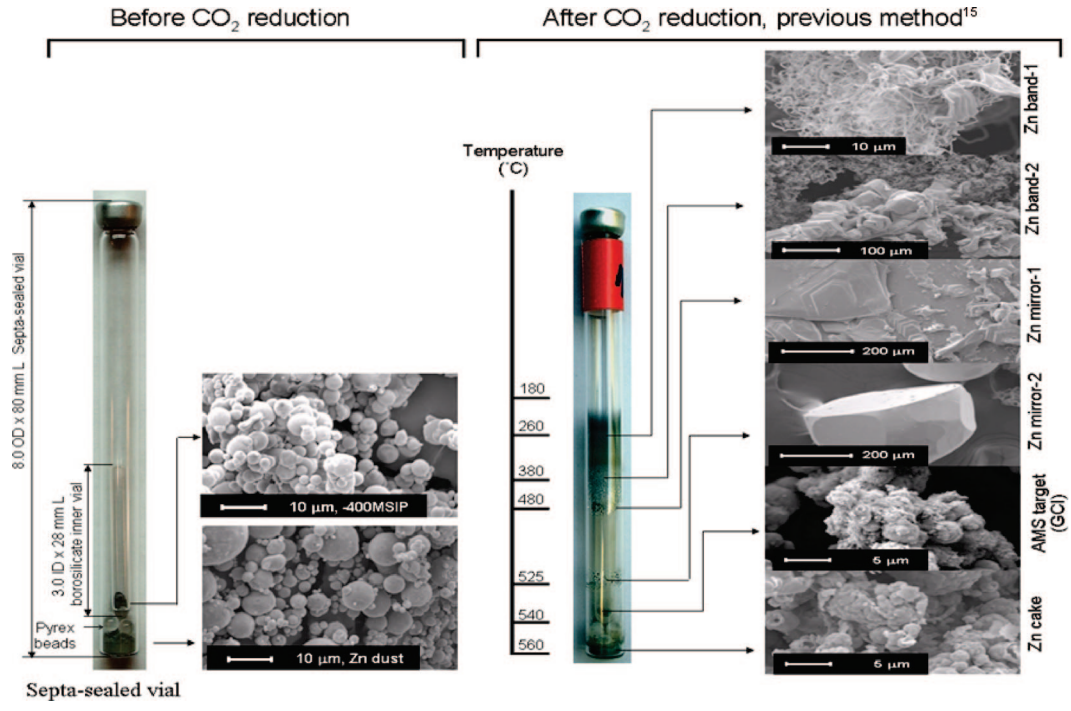

Figure 1. Overview of the reduction of CO_2 to graphite by our previous graphitization method,[15] which used ~100 mg of Zn dust (a reductant), ~10 mg of −400MSIP (a catalyst), and 525 °C (average temperature, 2 cm from bottom) for 6 h. The reduction temperature varied from 480 ± 7 (top Cu heating plate) to 560 ± 7 °C (bottom Cu heating plate). During the reduction, the Zn dust was converted to Zn cake (right bottom SEM), two Zn mirrors (right two middle SEMs) plus two Zn bands (right two top SEMs), and the graphite-coated Fe (GCI) as a fuzz (right the second SEM from the bottom).

The F_m of a sample of interest was the ratio of $(^{14}C/^{13}C)_{sample}/(^{14}C/^{13}C)_{Ox\text{-}2}$, each normalized for $\delta^{13}C$. The $\delta^{13}C$ was calculated as $[(^{13}C/^{12}C)_{sample} - (^{13}C/^{12}C)_{PDB}]/(^{13}C/^{12}C)_{PDB} \times 1000$, where PDB referred to the Cretaceous belemnite formation at Peedee, SC.[19] The $\delta^{13}C$ value used in this study was −25 ‰ for biological/biomedical application and −17.8 ‰ for Ox-2 SRM. Four C sources were compared using our previous method[15] and our optimized method.

Graphite quality was also examined using scanning electron microscopy (SEM) with a Philips XL30 (FEI Co., Hillsboro, OR) set at 15-kV accelerating energy and 5 spot size. The graphite-coated catalysts (Fe or Co) were sputtered 3 times with a thin

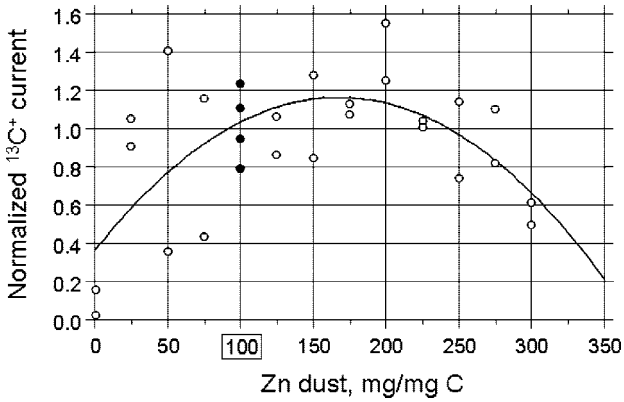

Figure 2. Plot of $n^{13}C^+$ current according to the quantity of Zn. (Our previous method was represented by full circles that correspond to 100 mg of Zn.) We confirmed previous findings that the 100 mg of Zn was optimal (abscissa solid rectangle).[15] The regression equation was $y = 0.3589 + 0.0096x - 0.00003x^2$, $r = 0.635$.

film of gold under <30 mA by Pelco Auto Sputter Coater SC7 (Ted Pella Inc., Redding, CA) before SEM imaging. SEM pictures enabled us to characterize the graphite that coated ("with a fuzz") or covered ("with a fluff") the surface of the metal catalyst under different reduction conditions so that those characteristics could be correlated with the highest, most reliable, and stable $n^{13}C^+$ current from the AMS. The coated "fuzz" on the surface of the metal catalyst adhered more strongly than the covered "fluff". This difference is important because the "fuzz" does not fall/separate from the metal catalyst as the target is transferred and tamped into the AMS target holder.

Finally, the data were analyzed using analysis of variance, and differences between our previous and our optimized methods were evaluated using Fisher's PLSD.

RESULTS

Figure 1 presented an overview of the second step of AMS target preparation. The left panel shows the setup and appearance of the zinc dust reductant and the −400MSIP catalyst before the CO_2 was reduced. The right panel shows the appearance of the zinc and the −400MSIP after the CO_2 was reduced using our previous method.[15] After the CO_2 was transferred to the septa-sealed vial but before it was reduced, the Zn dust consisted of loose spherical particles, while after reduction, the Zn dust was deformed and sintered. During the reduction, Zn dust was converted to (1) two Zn bands in the coolest regions of the septa-sealed vial (Zn band-1 at 260 °C and Zn band-2 at 380 °C), (2) two Zn mirrors in a warmer region (Zn mirror-1 at 480 °C and Zn mirror-2 at 525 °C), and (3) a hard Zn cake at 560 °C that stuck to the bottom of the septa sealed vial. Zn band-1 appeared fibrous (rubbery), while Zn band-2 appeared plasticized or plastic-like. Zn mirror-2 appeared to have a crystal structure and stuck to the septa-sealed vial. Finally, the −400MSIP appeared as a fuzz of GCI rather than being covered with a fluff of graphite which upon shaking fell off.

Figure 2 plotted the $n^{13}C^+$ current according to the quantity of Zn dust being used (per mg of C) for the reduction step. The highest $n^{13}C^+$ current was experienced when the quantity of Zn dust was in the range of 100−250 mg of Zn dust, so we considered the 100 mg of Zn dust as optimal. When ≥150 mg of Zn dust was used, the excess graphite began to coat over the Zn as Zn bands and mirrors (instead of the −400MSIP), thereby decreasing the graphitization yield and increasing isotopic fractionation. The Zn band-1 and Zn band-2 tended to fall atop the AMS target in the borosilicate inner vial, inadvertently contaminating the AMS target, and thereby reducing the $n^{13}C^+$ current. When <100 mg of Zn dust/mg of solid source C was used, ICM was formed depending on the temperature and mass of iron catalyst.

Figure 3 summarized SEM pictures before and after the reduction of CO_2, the $n^{13}C^+$ current, and the F_m values after the reduction of CO_2, when 10 mg each of three Fe catalysts or two Co catalysts was used along with 100 mg of Zn at 525 °C for 6 h. The −400MSIP had a uniform coat of graphite, the strongest and most reliable $n^{13}C^+$ current, and the most accurate and precise F_m values (histograms), so we ranked the −400MSIP as the best catalyst. The −325 mesh H_2-reduced Fe, the −50/+100 mesh H_2-reduced Fe, and the −100 mesh Co (cracked egg shell-like-Co) were loosely covered with a fluff of graphite. The −325 mesh irregular Co was covered with filamentous graphite (FG). Because all five catalysts, except for the −400MSIP, did not coat uniformly with graphite, their respective $n^{13}C^+$ current and F_m values were weak and variable.

Figure 4 summarized the SEM pictures and $n^{13}C^+$ current to quantity the −400MSIP used. In general, quantities of the −400MSIP in the range of 5−8 mg yielded the strongest $n^{13}C^+$ current and were uniformly coated with a fuzz of graphite, so we choose 5 mg of −400MSIP as optimum. When a small amount of −400MSIP (1 mg) was used, it was heavily (and loosely) coated with graphite (left SEM picture), and the excess graphite appeared as Zn band-1 and Zn band-2 that contaminated the AMS target thereby lowering the $n^{13}C^+$ current. When a large quantity (10 mg) of −400MSIP was used, it was coated with too little GCI or ICM. ICM was possibly an iron carbide (Fe_3C) instead of graphite (right SEM picture).

Figure 5 summarized SEM pictures, $n^{13}C^+$ current, and F_m values according to the three reduction temperatures/mg of C listed. The left SEM picture showed that the 500 °C temperature produced a uniform coat of a fuzz of graphite, while the 525 or 550 °C temperatures produced a crustlike cover of graphite. At 500 and 525 °C, the $n^{13}C^+$ currents were reliable and F_m values were accurate and precise. At 500 °C, a uniform coat of graphite was produced 100% of the time while 525 °C produced ICM 20% of the time instead of graphite. As reduction temperature increased, more sinter of the −400MSIP occurred, which led to isotopic fractionation, thus underestimating the F_m values.[20,21] Also, septa sealed vials begin to melt at 600 °C. Finally, at 550 °C, the F_m value of the Ox-2 SRM was underestimated (1.3151 ± 0.0128 versus 1.3407[16]). Therefore, we considered 500 °C as optimal.

Figure 6 summarized SEM pictures and $n^{13}C^+$ current according to duration (up to 6 h) of heating at 525 °C. In general, the

(17) Snyder, W. S.; Cook, M. J.; Nasset, E. S. *Report of the task group on reference man ICRP publication 23*; Pergamon Press: New York, 1975.
(18) Harris, D.; Horwáth, W. R.; van Kessel, C. *Soil Sci. Soc. Am. J.* **2001**, *65*, 1853–1856.
(19) Donahue, D. J.; Linick, T. W.; Jull, A. J. T. *Radiocarbon* **1990**, *32*, 135–142.
(20) Chang, R. *Physical Chemistry for the Biosciences*, 3rd ed.; University Science Books: Herndon, VA, 2005.
(21) Xu, X.; Trumbore, S. E.; Zheng, S.; Southon, J. R.; McDuffee, K. E.; Luttgen, M.; Liu, J. C. *Radiocarbon* **2007**, *259*, 320–329.

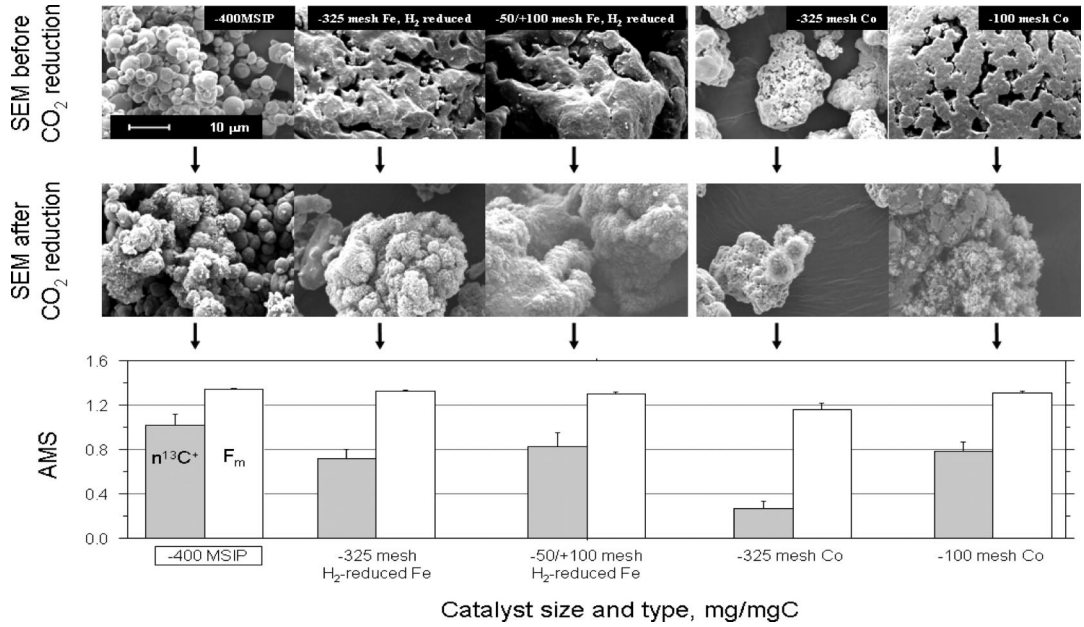

Figure 3. Before and after CO_2 reduction SEM pictures and the corresponding $n^{13}C^+$ currents and the F_m values of the Ox-2 SRM according to five different catalysts. [The $n^{13}C^+$ currents are represented by full bars and the F_m values by empty bars (means + SE, $n \geq 4$). We confirmed previous findings that the −400MSIP was optimal (abscissa solid rectangle) because it received a uniform coat of graphite fuzz (left SEM), which had the highest $n^{13}C^+$ current and accurate F_m values that best matched the accepted value (1.3407) of the Ox-2 (NIST SRM 4990C).][16]

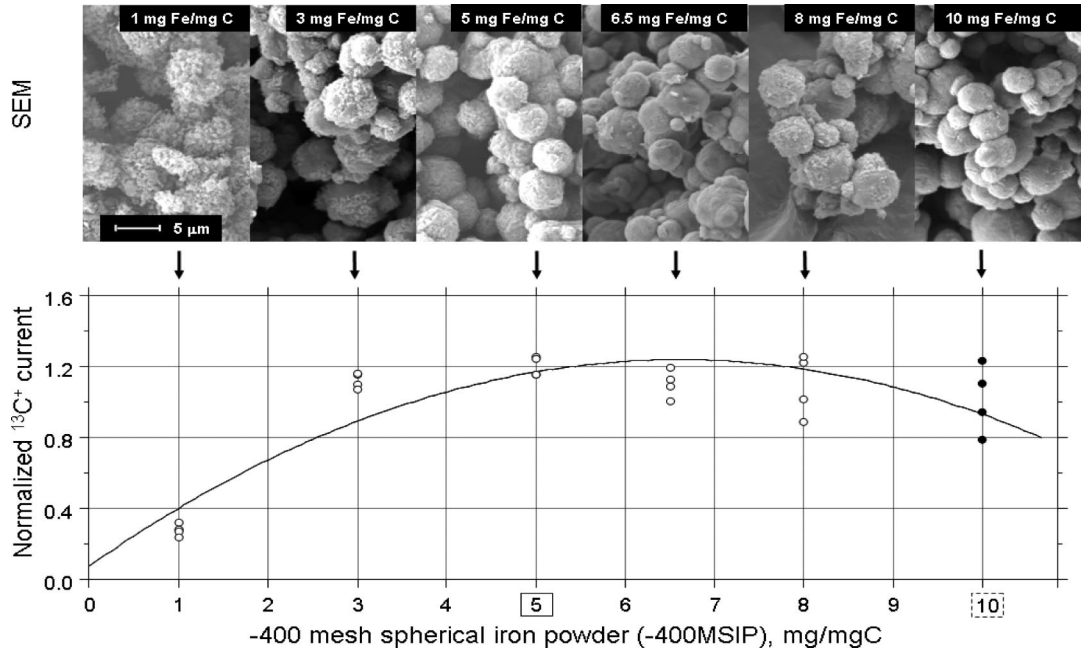

Figure 4. After CO_2 reduction SEM pictures and $n^{13}C^+$ currents according to the mass of −400MSIP used. [The full circles did not confirm previous findings (abscissa broken rectangle),[15] instead the 5-mg quantity of −400MSIP (abscissa solid rectangle) was coated with a uniform fuzz of graphite and was associated with the highest $n^{13}C^+$ current. The regression equation was $y = 0.0776 + 0.3516x - 0.0266x^2$, $r = 0.8661$.]

$n^{13}C^+$ current was independent of the duration of heating under these conditions (bottom panel). When the duration, the temperature, or both of the reduction step were insufficient or when the mass of the −400MSIP was not optimal, inaccurate F_m values were experienced apparently because the CO_2 reduction step was incomplete. Heating for 6 h at 525 °C (broken rectangle) was needed to minimize isotopic fractionation while heating for only 3 h at 500 °C (solid rectangle) also minimized isotopic fractionation with increased throughput, so it was considered as optimal.

Figure 7 compared the AMS targets' qualities using our previous[15] and our optimized methods. Our optimized method used 100 ± 1.3 mg of Zn dust, 5 ± 0.4 mg of −400MSIP, and 3 h reduction time at 500 °C, whereas our previous method[15] used ∼100 mg of Zn dust, ∼10 mg of −400MSIP, and 6 h reduction time at 525 °C. Our optimized method produced exclusively graphite-coated Fe powder (GCIP) 100% of the time. The GCIP consisted of a mix of a graphite fuzz plus small pieces of "graphite sheet" (right SEM picture), whereas our previous method[15]

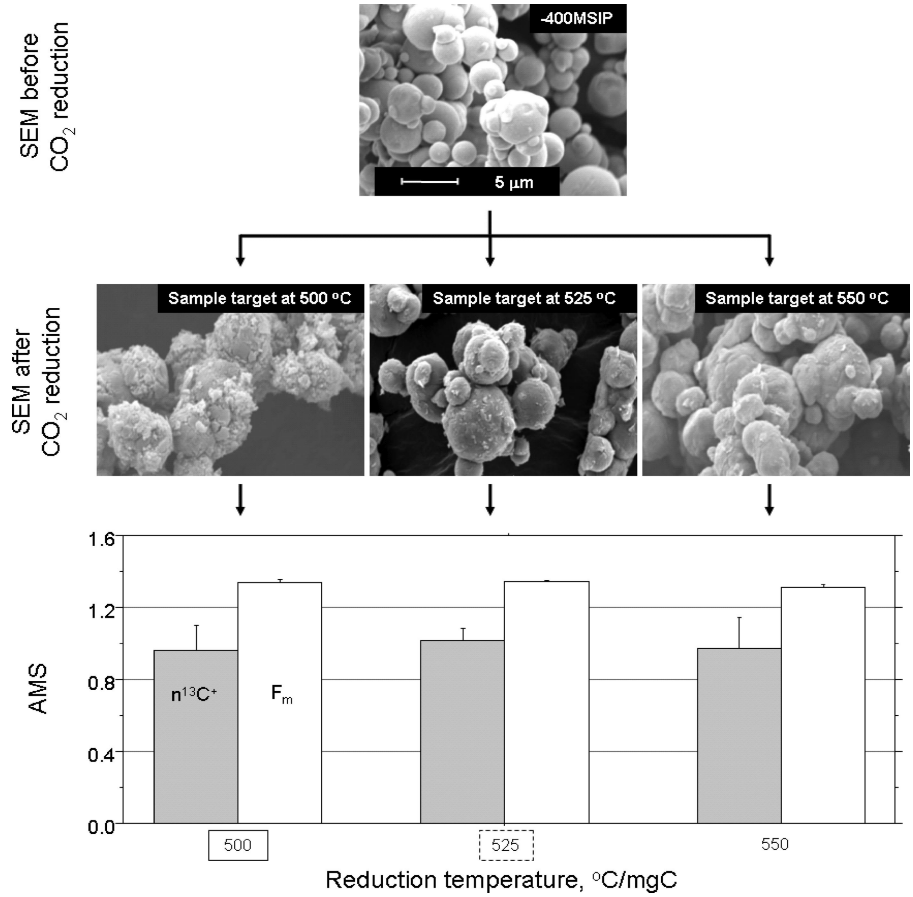

Figure 5. Before and after CO_2 reduction SEM pictures and the corresponding $n^{13}C^+$ currents and F_m values of the Ox-2 SRM according to reduction temperature. [The $n^{13}C^+$ currents are represented by full bars and the F_m values by empty bars (means + SE). The 500 °C temperature was optimal (abscissa solid rectangle) because it was the lowest temperature at which the −400MSIP received a uniform coat of graphite fuzz (left SEM) with the F_m values that best matched the theoretical value (1.3407) of the Ox-2 (NIST SRM 4990C).[16] The lowest temperature was important because at ~600 °C the septa-sealed vial begins to soften and melt.]

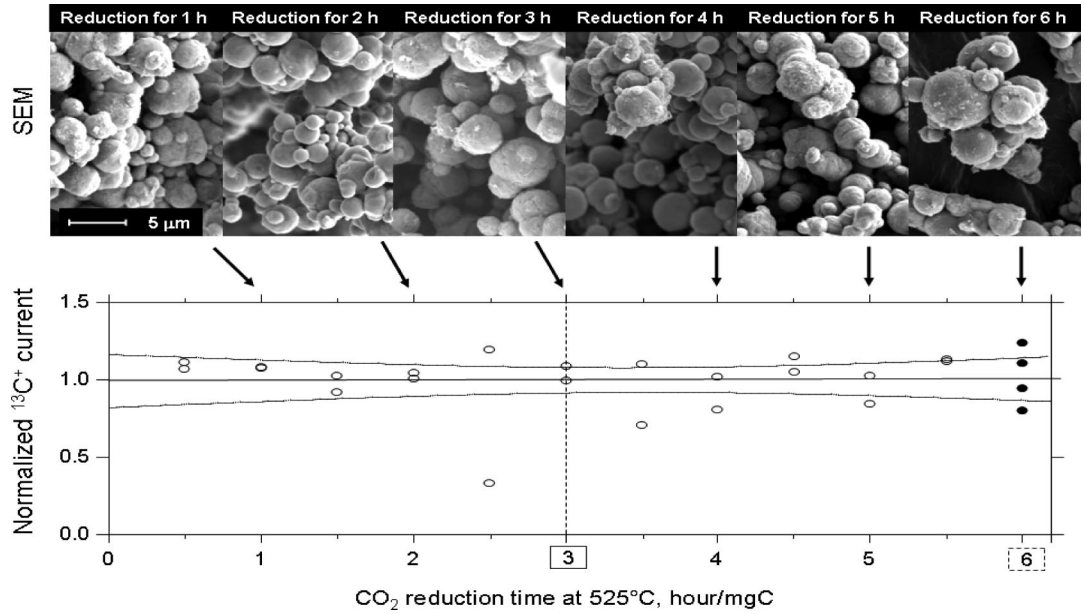

Figure 6. SEM pictures and the $n^{13}C^+$ currents according to the duration of heating (reduction) time (up to 6 h) using 100 mg of Zn dust, 10 mg of −400MSIP, and 525 °C used to reduce CO_2 to graphite (regression and 95% confidence interval belt). Under these conditions, reduction time was not a significant factor and the previous method[15] needed 6 h (abscissa broken rectangle). But we confirmed that 3 h was optimal (abscissa solid rectangle) based on the uniformity of the graphite coat when CO_2 was reduced at 500 °C (data not shown).

produced GCI, which was a nonuniform coat of graphite fuzz, only 80% of the time (left SEM picture). The GCIP produced higher $n^{13}C^+$ currents (~3%) and the F_m values that matched those of the Ox-2 SRM more closely than did our previous method[15] (F_m

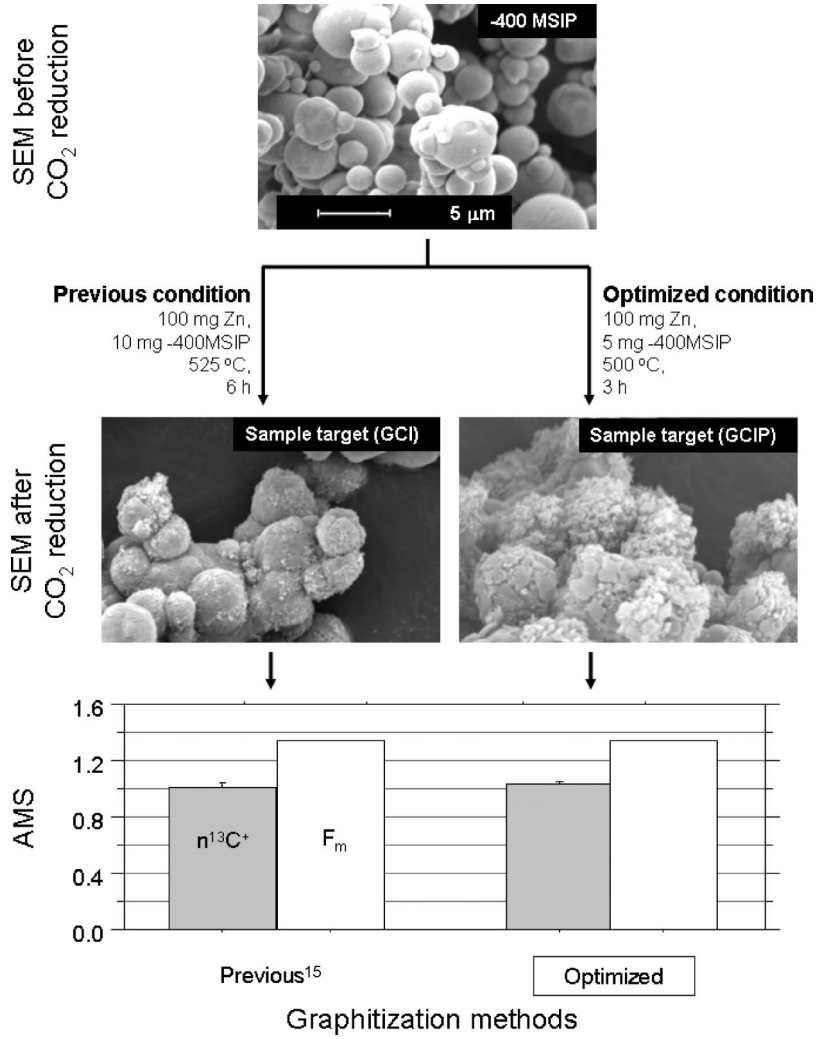

Figure 7. SEM pictures, the $n^{13}C^+$ currents, and F_m according to our previous method[15] that used 100 mg of Zn dust, 10 mg of −400MSIP, and 525 °C for 6 h to reduce CO_2 to GCI. The $n^{13}C^+$ currents are represented by full bars and the F_m values by empty bars (means + SE, SE < line thickness). Our optimized method (abscissa solid rectangle) differed by using only 5 mg of −400MSIP, and 500 °C for 3 h. Our optimized method ensured the CO_2 (from 1 mg of solid C) was uniformly and reliably converted to GCIP, which loaded easily into the AMS target holder. It maximized $n^{13}C^+$ current for accurate F_m values of solid C from many sources. The 500 °C temperature for 3 h assured the septa-sealed vials and Teflon cap did not soften/melt.

Table 2. F_m Values of Four Carbon Sources by Our Previous and Optimized Graphitization Methods[a]

	mean of F_m ± SE n = number of samples		
carbon source	our previous method[15]	our optimized method	p-value
oxalic acid II (Ox-2, NIST SRM 4990C)[b] accepted F_m value 1.3407[16]	1.3432 ± 0.0024 $n = 32$	1.3410 ± 0.0027 $n = 32$	0.5401
sucrose (ANU) consensus F_m value 1.5061 ± 0.001[21b]	1.5091 ± 0.0033 $n = 28$	1.5034 ± 0.0032 $n = 25$	0.2259
TRIB used to fortify HPLC fractions with C	0.0472 ± 0.0016 $n = 40$	0.0497 ± 0.0019 $n = 40$	0.3161
fasting human plasma	1.0482 ± 0.0050 $n = 63$	1.0609 ± 0.0023 $n = 35$	0.0716

[a] The limit of detection (LOD) and limit of quantification (LOQ) were determined using the tributryn.[22] The LOD was 0.04 amol and LOQ was 0.07 amol. The accuracy and precision between our previous and our optimized methods were compared using the Ox-2. The accuracy [relative error = (measured F_m − accepted F_m)/accepted $F_m \times 100$] was 0.022% using our optimized method compared to 0.187% using our previous method, while the precision (RSD (relative standard deviation) = SD of measured F_m/mean of measured $F_m \times 100$) was 1% for both methods. [b]The 1 mg of C from Ox-2 or ANU sucrose was oxidized to CO_2 and then reduced to graphite by our previous[15]and optimized methods.

values are detailed in Table 2). In addition, our optimized method avoided formation of the ICM, which produced $n^{13}C^+$ currents and F_m values that were low and variable. Finally, the GCIP was also much easier to tamp into AMS target holders.

Figure 8 summarized the relationship of $^{13}C^+$current and of $n^{13}C^+$ current to the F_m values. The "y axis" represented the

(22) Vogel, J. S.; Grant, P. G.; Buchholz, B. A.; Dingley, K.; Turteltaub, K. W. *Electrophoresis* **2001**, *22*, 2037–2045.

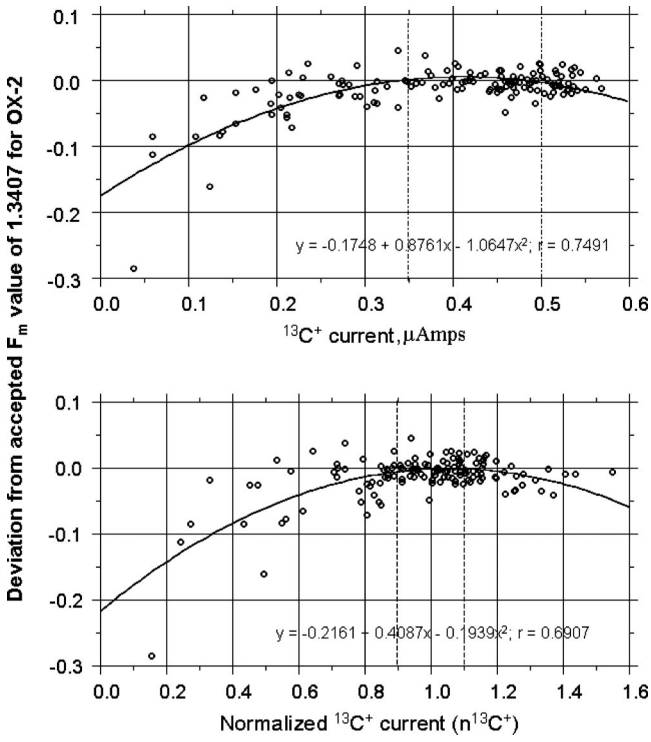

Figure 8. Relationship of $^{13}C^+$current and of $n^{13}C^+$ current to the F_m values. [The deviation of F_m value was calculated as the accepted F_m value (1.3407) of Ox-2 was subtracted to measured F_m value of Ox-2 by our previous and optimized methods (numer of samples, n = 149). A zero value means that accepted and measured F_m values were identical. The vertical dashed lines are reliable ion current ranges for accurate F_m values.]

difference between the accepted F_m value (1.3407) and the measured F_m values for the Ox-2 (NIST SRM 4990C) using our previous[15] and our optimized methods. A difference of zero meant that accepted and measured values were identical. The $^{13}C^+$ currents in the range of 0.35−0.5 μA guaranteed accurate ^{14}C measurement (top panel, dashed vertical lines). The $n^{13}C^+$ currents in the range of 0.9−1.1 were adequate for accurate ^{14}C measurement (bottom panel, dashed vertical lines). For $^{13}C^+$ current outside the 0.35−0.5 μA range, the F_m values can be underestimated by as much as 20% and can be variable.

Table 2 compared the F_m values of four C sources as measured by our previous[15] and our optimized method in the present paper. Respective values for the Ox-2 SRM and the ANU sucrose match their accepted and consensus F_m values demonstrating the accuracy of our previous and our optimized methods. The relative error (accuracy) was 0.022% using our optimized method compared to 0.187% using our previous method,[15] while the precision was 1% for both methods. The LOD and LOQ were determined using the tributyrin.[22] The LOD and LOQ were 0.04 and 0.07 amol, respectively. The mean F_m values between our previous method[15] and optimized method for any of the four C sources was not significant ($p < 0.05$) and our optimized method took only half a second to complete as our previous method. It was important that our optimized method be reliable for production of high-quality graphite in less than half the time of our previous method.[15]

DISCUSSION

In general, intense ion current, >100 μA $^{12}C^-$/mg of solid source C, was required for high sample throughput and accurate F_m in biological/biomedical applications of AMS.[11,23] Our previous method[15] produced AMS targets of GCI 80% of the time and of ICM 20% of the time. AMS targets of GCI produced intense ion currents of ∼115 μA $^{12}C^-$/mg of solid source C. On the other hand, AMS targets of ICM produced $^{12}C^-$ currents of only 100 μA $^{12}C^-$/mg of solid source C, which led to low and variable F_m values. A possible reason why ICM produced weak $^{12}C^-$ current was that the ICM might be iron carbide (mostly Fe_3C with traces of Fe_xC_y). Cobalt carbide produced lower ion current than did graphite, which resulted in a 5−10% error in the F_m.[12] AMS targets of ICM were also difficult to tamp into the AMS target holder. Therefore, our objective was to examine the experimental conditions of the second step of AMS target preparation where CO_2 transferred to a septa-sealed vial was reduced to high-quality graphite for the intense ion current required for accurate measurements of F_m with high throughput for biological/biomedical applications of AMS. Biological/biomedical applications involved F_m values in the range of 0.01−100 or isotope ratios in the range of 10^{-14}−10^{-10} compared to ratios of 10^{-15}−10^{-12} for carbon dating.[10,24] Adequate quantities of solid C source are almost always present in samples for biological/biomedical AMS, whereas small quantities of solid C source are present in samples for carbon dating.

Effect of the amount of Zn dust. The amount of Zn dust was one of the critical factors for the formation of high-quality graphite because it generated a H_2 reductant and converted CO_2 to CO during the reduction step (Table 3, eqs 1 and 2). Generally, excess Zn was undesirable because it led to the formation of thicker Zn bands and Zn mirrors on the inside of the septa-sealed vial during the reduction of CO_2. Higher reduction temperature and longer reduction duration produced thicker bands and mirrors.[25]

Some of the Zn bands and the Zn mirrors fell atop the AMS targets in the borosilicate inner vial of the septa-sealed vial and were inadvertently transferred onto (contaminating) the AMS target and decreased sputtering yields in the AMS ion source. Furthermore, when the ratio of the mg of Zn dust/mg of solid C source was in excess, graphite began to coat over the Zn instead of the Fe, thereby decreasing the graphite yield, and increasing isotopic fractionation. It was reported previously that 75−150 mg of Zn/mg of solid C source maximized the $^{13}C^+$ current.[14] While ∼175 mg of Zn dust maximized the $n^{13}C^+$ current (Figure 2), it also resulted in a thicker Zn band, which reduced the inside diameter of the septa-sealed vials, which in turn made it more difficult to retrieve the inner vial (containing the AMS target). At 100 mg of Zn dust, the $n^{13}C^+$ current was still reliable, the F_m measurement was still accurate and precise, and the thickness of the Zn band allowed for the inner vial (containing the AMS target) to be easily retrieved from the septa-sealed vial. At <100 mg of Zn dust/mg of solid source C, ICM was formed depending on the quantity of iron catalyst or the reduction temperature used.

The $n^{13}C^+$ current obtained by using 100 mg of Zn dust confirmed the previous findings[15] that the 100 mg of Zn dust was optimal because it produced reliable $n^{13}C^+$ current, so we considered 100 mg of Zn dust as optimal. Once the quantity of

(23) Ognibene, T. J.; Bench, G.; Brown, T. A.; Peaslee, G. F.; Vogel, J. S. *Int. J. Mass Spectrom.* **2002**, *218*, 255–264.
(24) Vogel, J. S.; Love, A. H. *Methods Enzymol.* **2005**, *402*, 402–422.
(25) Wilson, A. T. *Radiocarbon* **1992**, *34*, 318–320.

Table 3. Chemical Reactions during the Reduction Portion of Graphitization Process by Zn Reduction Method

		ΔG_{temp} (kJ·mol^{-1})[b]					
eq no.	reduction reaction of CO_2	298 K (25 °C)	723 K (450 °C)	773 K (500 °C)	798 K (525 °C)	823 K (550 °C)	873 K (600 °C)
1	$CO_{2(g)} + Zn_{(s)} \rightleftharpoons CO_{(g)} + ZnO_{(s)}$	−61.2	−55.6	−54.9	−54.6	−54.3	−53.5
2	$H_2O_{(g)} + Zn_{(s)} \rightleftharpoons H_{2(g)} + ZnO_{(s)}$	−89.7	−65.7	−62.9	−61.5	−60.1	−57.3
3	$CO_{2(g)} + H_{2(g)} \overset{Fe}{\rightleftharpoons} CO_{(g)} + H_2O_{(g)}$	+28.5	+10.4	+8.3	+7.2	+6.1	+4.0
4	$CO_{(g)} + H_{2(g)} \overset{Fe}{\rightleftharpoons} C_{gr(s)}$[a] $+ H_2O_{(g)}$	−91.3	−34.3	−27.5	−24.2	−20.8	−14.1
5	$2CO_{(g)} \overset{Fe}{\rightleftharpoons} C_{gr(s)} + CO_{2(g)}$	−119.8	−44.6	−35.8	−31.4	−27.0	−18.1
6	$CO_{2(g)} + 2H_{2(g)} \overset{Fe}{\rightleftharpoons} C_{gr(s)} + 2H_2O_{(g)}$	−62.8	−23.9	−19.3	−17.0	−14.7	−10.1
7	$CO_{(g)} + H_2O_{(g)} \rightleftharpoons H_{2(g)} + CO_{2(g)}$	−28.5	−10.4	−8.3	−7.2	−6.1	−4.0
8	$2CO_{(g)} + 2H_{2(s)} \overset{Fe}{\rightleftharpoons} CH_{4(g)} + CO_{2(g)}$	−170.6	−61.1	−48.23	−41.8	−35.4	−22.5
9	$CO_{(g)} + 3H_{2(g)} \overset{Fe}{\rightleftharpoons} CH_{4(g)} + H_2O_{(g)}$	−142.1	−50.7	−40.0	−34.6	−29.2	−18.5

[a] Graphite-coated Fe (called graphite). [b] The thermodynamics of CO_2 reduction was predicted using the following equation $(\Delta_r G°/T)_{T2} = (\Delta_r G°/T)_{T1} + \Delta_r H°(1/T_2 - 1/T_1)$ derived from the Gibbs−Helmholtz equation. (See Supporting Information available.)

Zn dust was optimized, the type, particle size, and quantity of catalysts were then optimized.

Effect of Catalyst Type and Particle Size. During the reduction step using Zn dust, the CO or CO_2 was reduced to graphite over a transition metal (iron or cobalt) surface (Table 3, eqs 4−6). Spherical-shaped metal catalysts formed graphite more slowly than did dendritic or irregular-shaped metal catalysts. Also metal powders larger than 150 mesh (100 μm) reacted slowly, so the −200 mesh spherical Fe and the −325 mesh spherical Co were preferred catalysts.[26,27] The presence of sulfur or nitric oxide at the catalyst interface was detrimental to carbon deposition onto catalysts.[28] Finally, the pretreatment of the −325 mesh spherical Fe by oxidation and reduction produced much more graphite compared to nontreated catalysts.[29]

An evaluation of catalyst suitability for AMS revealed that Alfa-Aesar's −325 mesh Fe formed FG, which did not affect the C^- current intensity or background and was easy to pack into the AMS target holders.[30] Furthermore, the SEM pictures in Figure 3 were consistent with prior SEM pictures of graphite formation when −325 mesh H_2-reduced Fe or −325 mesh Co but not when −400MSIP (left SEM picture in Figure 3) was used.[30] The difference may be associated with the formation of solid graphite on the −400MSIP[30] that occurred with increased Fe sintering when the reduction step was conducted at temperatures of >525 °C.

Effect of Catalyst Quantity per Milligram of Solid Source C. A prior study has shown that a 15:1 ratio of Fe/solid C source fused the graphitized iron into a bead.[31] A smaller ratio frequently resulted in immiscible Fe−C mixtures, while larger ratios lead to smaller C^- currents. In general, ratios of Fe/C of 2:1 to 3:1 produced an abundance of fluffy graphite, larger ratios tended to permeate the Fe with carbon to form iron carbide instead of graphite, and extreme ratios (Fe/C of 15:1) fused the graphitized iron into a bead.[31] Our previous method[15] formed GCI 80% of the time, which produced reliable ion currents and accurate F_m values for various solid C sources. Our previous method[15] also produced some ICM 20% of the time. The occasional production of ICM may be due to the use of the larger ratio of Fe/C compared to prior studies.[27,32,33] Powder X-ray diffraction (PXRD) analysis of the ICM revealed a crystal structure characteristic of iron carbide (Fe_3C) rather than graphite (see Figure 5 in part 2), whereas XRD analysis of the GCI and GCIP also revealed a Fe_3C crystal and possibly a disordered carbon structure. Furthermore, FT-IR analysis revealed a C=C bond stretching for GCI and GCIP but not one for ICM (see Figure 3 in part 2). Therefore, we considered the 5 mg of −400MSIP as optimal because this smaller ratio of Fe/C minimized production of ICM.

Effect of Reduction Temperature and Time. Above 750 °C, graphite formation did not occur because the −400MSIP was deformed (inactivated). Below 500 °C, production of hydrocarbon by Fischer−Tropsch reaction (Table 3, eqs 8 and 9) was favored over graphite especially at H_2/CO ratios >3:1.[26,31,32] As the temperature of the reduction step increased, the balance of the forward reactions in eqs 4−6 in Table 3 became less favorable thermodynamically but more favorable kinetically.[31] The data in Table 3, eqs 1 and 5, confirmed prior work that the most favorable (thermodynamically) reduction occurred at 600 °C when using the modified Zn reduction method.[34] When the H_2 or the Zn reduction method was used, the rate of carbon deposition ranged from 0.2 to 0.4 mg of C/h within the temperature range of 500−650 °C.[7,26] Formation of graphite in 3 h at 500 °C by our optimized method was consistent with prior reports that graphite formation can be >95% completed in 1 h at 600 °C[35] to 4 h at 500 °C.[14] The formation of graphite in 3 h at 500 °C was also important for two reasons. First, at ≥600 °C, our septa-sealed Pyrex vials and Teflon (caps) melt, and second, at <450 °C, carbon samples were converted to methane.[31] Although 525 °C was preferred

(26) Vogel, J. S.; Southon, J. R.; Nelson, D. E.; Brown, T. A. *Nucl. Instrum. Methods Phys. Res., Sect. B* **1984**, *5*, 289–293.
(27) Vogel, J. S.; Southon, J. R.; Nelson, D. E. *Nucl. Instrum. Methods Phys. Res., Sect. B* **1987**, *29*, 50–56.
(28) Thomsen, M. S.; Gulliksen, S. *Radiocarbon* **1992**, *34*, 330–334.
(29) Hua, Q.; Zoppi, U.; Williams, A. A.; Smith, A. M. *Nucl. Instrum. Methods Phys. Res., Sect. B* **2004**, *223−224*, 284–292.
(30) Santos, G. M.; Mazon, M.; Southon, J. R.; Rifai, S.; Moore, R. *Nucl. Instrum. Methods Phys. Res. Sect. B* **2007**, *259*, 308–315.
(31) Verkouteren, R. M.; Klouda, G. A. *Radiocarbon* **1992**, *34*, 335–343.
(32) Dee, M.; Ramsey, C. B. *Nucl. Instrum. Methods Phys. Res., Sect. B* **2000**, *172*, 449–453.
(33) D'Elia, M.; Calcagnile, L.; Quarta, G.; Sanapo, C.; Laudisa, M.; Toma, U.; Rizzo, A. *Nucl. Instrum. Methods Phys. Res., Sect. B* **2004**, *223−224*, 278–283.
(34) Verkouteren, R. M.; Klouda, G. A.; Currie, L. A.; Donahue, D. J.; Jull, A. J. T.; Linick, T. W. *Nucl. Instrum. Methods Phys. Res., Sect. B* **1987**, *29*, 41–44.
(35) Ramsey, C. B.; Hedges, R. E. M. *Nucl. Instrum. Methods Phys. Res., Sect. B* **1997**, *123*, 539–545.

thermodynamically in our previous method,[15] it still needed 6 h to avoid larger isotopic fractionation for accurate AMS measurement. Therefore, we concluded that 500 °C for 3 h was optimal to maximize sample throughput with reliable $n^{13}C^+$ current and accurate F_m measurement.

Comparison of our Previous[15] and Our Optimized Methods. Key factors that influence the formation and quality of graphite include the catalyst size, the mass ratio of Fe/solid source C, and the reduction temperature and time. In general, <500 °C was the preferred temperature for conversion of CO_2 to CO whereas >500 °C was preferred for deposition of CO as graphite.[31,34] The change of Gibbs's energy with respect to temperature can be estimated using Gibbs−Helmholtz equation ($[\partial(\Delta G/T)/\partial T]_p = -\Delta H/T^2$) and thermodynamic data at 1 bar and 298 K, whereas kinetic energy must be experimentally determined. Results of this calculation confirmed prior estimates[31,34] except in eq 3 (Table 3) where all forward reactions were spontaneous, although the kinetics was slow at low temperatures. Methane formation was not a problem at 500 to 600 °C with lower H_2 concentration whereas formation of iron carbonyl ($Fe(CO)_5$) was not spontaneous in that temperature range. Graphite formation was less favored thermodynamically at high temperature in eqs 4−6 (Table 3) because of entropy but became more kinetically favored due to diminished activation energy of reactions ($k = Ae^{-E_a}/RT$). In our present study, 500, 525, and 550 °C were thermodynamically favored, but CO_2 reduction time at 500 °C was shorter than at 525 and 550 °C because it had less sinter of the Fe catalyst (−400MSIP). Use of 1−5-μm-sized powders did not increase the reaction rate due to sintering;[26] instead, our optimized method produced a uniform GCIP (<37 μm, i.e., ∼5 μm size). Our optimized method had less sinter of the −400MSIP by using a combination of 500 °C and 5 mg −400MSIP per mg of solid C source indicating that our optimized method at 500 °C was more favorable thermodynamically for graphitization over our previous method.[15] Ninety percent of the carbon in the sample of interest was recovered as graphite using our previous[15] and optimized methods. The $\delta^{13}C$ of 1-mg aliquots of solid C was −18.4 ± 0.2‰ by our previous method[15] and was −17.9 ± 0.3‰ by our optimized method, and the $\delta^{13}C$ especially by the optimized method was within the accepted range (−17.8 ± 0.05‰).[16] Samples with 0.3−1 mg of C consistently produced high-quality graphite with high throughput using our optimized method.

Graphite quality (uniform coat of fuzz or filamentous graphite) affected the ionization efficiency and ion currents. We focused on high-quality graphite to consistently produce reliable $^{13}C^+$ current, $n^{13}C^+$ current, and F_m values for the Ox-2 SRM that were accurate and precise. The 1-mg aliquots of solid C source produced a reliable $^{13}C^+$ current of 0.35−0.5 μA, which corresponded to a $^{12}C^+$ current of 0.9−1.1 or to a C^- current of ∼115 μA. Intense ion currents in these ranges guaranteed accurate F_m values with high throughput for biological/biomedical applications of AMS[11,23] despite a recent report[36] that the ratio of $^{14}C/^{12}C$ was independent of ion currents.

CONCLUSIONS

We optimized the reduction step by using 100 mg of Zn dust, 5 mg of −400MSIP, and 500 °C for 3 h to produce exclusively high-quality AMS targets for biological/biomedical application of AMS. Our optimized CO_2 reduction method was thermodynamically more favorable than our previous method. Consequently, throughput was doubled, graphitization yield was ≥90%, $\delta^{13}C$ of Ox-2 SRM was −17.9 ± 0.3‰, LOD was 0.04 amol, LOQ was 0.07 amol, relative error was 0.022%, and precision was 1%.

ACKNOWLEDGMENT

The authors thank the reviewers for their perceptive and helpful comments. The authors also thank Drs. Ted Ognibene and Bruce Buchholz at LLNL CAMS for AMS measurements. This work was supported by NIH DK-45939, DK-48307, and the USDA Regional Research W-143 from the California Agricultural Experiment Station. SEMs were made at the Pathology Department, UCDMC. Graphitization yield and isotopic fractionation was measured by Dr. David Harris at Stable Isotope Facility, Plant Science Department, UCD. This work was performed in part under the auspices of the U.S. Department of Energy by the University of California-Lawrence Livermore National Laboratory under Contract W-7405-Eng-48 and NIH National Center for Research Resources Grant RR13461.

SUPPORTING INFORMATION AVAILABLE

Additional information as noted in text. This material is available free of charge via the Internet at http://pubs.acs.org.

Received for review June 16, 2008. Accepted August 8, 2008.

AC801226G

(36) Santos, G. M.; Southon, J. R.; Griffin, S.; Beaupre, S. R.; Druffel, E. R. M. *Nucl. Instrum. Methods Phys. Res., Sect. B* **2007**, *259*, 293–302.